

# Automated fish cage net inspection using image processing techniques

ISSN 1751-9659  
Received on 6th December 2019  
Revised 18th April 2020  
Accepted on 1st June 2020  
E-First on 6th July 2020  
doi: 10.1049/iet-ipr.2019.1667  
www.ietdl.org

Stavros Paspalakis<sup>1</sup>, Konstantia Moirogiorgou<sup>1</sup> ✉, Nikos Papandroulakis<sup>2</sup>, George Giakos<sup>3</sup>, Michalis Zervakis<sup>1</sup>

<sup>1</sup>School of Electrical & Computer Engineering, Technical University of Crete, University Campus, 73100 Chania, Crete, Greece

<sup>2</sup>Institute of Marine Biology, Biotechnology and Aquaculture, Hellenic Centre for Marine Research, Thalassocosmos, P.C. 71500, Gournes Heraklion, Crete, Greece

<sup>3</sup>Department of Electrical and Computer Engineering, Science and Technology Integration Research Laboratory, Manhattan College, Riverdale, NY, USA

✉ E-mail: dina@display.tuc.gr

**Abstract:** Fish-cage dysfunction in aquaculture installations can trigger significant negative consequences affecting the operational costs. Low oxygen levels, due to excessive fouling's, leads to decrease growth performance, and feed efficiency. Therefore, frequent periodic inspection of fish-cage nets is required, but this task can become quite expensive with the traditional means of employing professional divers that perform visual inspections at regular time intervals. The modern trend in aquaculture is to take advantage of IT technologies with the use of a small-sized, low-cost autonomous underwater vehicle, permanently residing within a fish cage and performing regular video inspection of the infrastructure for the entire net surface. In this study, we explore specialised image processing schemes to detect net holes of multiple area size and shape. These techniques are designed with the vision to provide robust solutions that take advantage of either global or local image structures to provide the efficient inspection of multiple net holes.

## 1 Introduction

With the term 'commercial aquaculture' we refer to the industry of intensive fish farming, where the term farming implies all actions necessary to secure a robust fish rearing process to achieve high rates of production and food quality. The infrastructure of aquaculture consists of floating underwater fish cages, where sufficient oxygen supply is one of those conditions to be satisfied, fresh water and food to the fish population. The growth of aquaculture [1] becomes so significant in recent years that makes it imperative to take actions that guarantee the sustainability of the structures. It is clear that maintenance actions must take place in a regular and efficient basis to restrain faults and, as a consequence, minimise the overall operational cost of the facilities.

Fish escapes from net holes, decreased growth performance or feed efficiency, as a result of low oxygen levels due to excessive fouling, are just a few of the most common problems. Furthermore, the recent trend in aquaculture is to move its activities away from the shore, to avoid competition from other users of the coastal zone, to increase farming sites and to reach more suitable environmental conditions. This trend increases the inspection costs, due to the additional transportation and delay demands, while frequent inspections are still required.

The advances in IT technologies offer a variety of additional inspection solutions, such as static submerged cameras, Remotely Operated Vehicle (ROV) and other sensors, capable of transmitting almost real-time information to the land-based facilities. Although these solutions certainly facilitate the operational procedures, they do require constant human involvement for their operation, which is associated with increased delays and costs. To overcome the manual inspection, the evident solution is to engage automated schemes with the use of autonomous underwater vehicle (AUV), permanently residing within a fish cage and performing regular inspection of the infrastructure [2, 3]. The mission of such an AUV is to record annotated video from the total net-surface and upload the video to a land-based server. Dedicated software can be deployed to analyse the video and automatically scan it for

problematic areas (e.g. net holes, excessive fouling). Upon successful detection, the position of the area, in terms of the inspection date, depth and bearing, as well as a relevant image are reported to the appropriate channel, with appropriate notifications (email, sms etc.). Nevertheless, the inspection methodology must handle diverse problems stemming from the underwater conditions, such as the blurred and obscure imaging due to the lighting conditions that vary with the day time or the season, the changing zoom recording due to the varying distance from the net, the mixed views of the net with overlaid fish, other floating structures etc. Thus, the software operation in a robust and efficient way is of utmost importance, rendering the specific application context quite different from other inspection areas.

In our study, we focus on the detection of fish cage net holes of different size and shape, since their presence must be handled fast and efficiently. We explore several circumstances of capturing the fish cage net under the water, with varying structure deformation and position. As a consequence, we test our methods on conditions that illustrate net cells with multiple combinations of translation, rotation and resize. In particular, the images used in this study for demonstration purposes represent net cases with differences regarding the size and the shape of holes, while in particular cases the appearance of some net cell boundaries is motion deformed due to water currents.

The rest of the paper is organised as follows: In Section 2, the state-of-the-art is presented regarding both the technologies for fish cage infrastructure inspection and the image processing techniques applied for the detection of net malfunction. In Section 3, we present the proposed image processing approach that is developed and implemented aiming first at global (abstract) and then at the local (detailed) search for the net structure. Finally, the outcome of our study is summarised in Section 4.

## 2 State-of-the-art

According to the FAO handbook of aquaculture operations in floating HDPE cages [4], the default way to monitor underwater

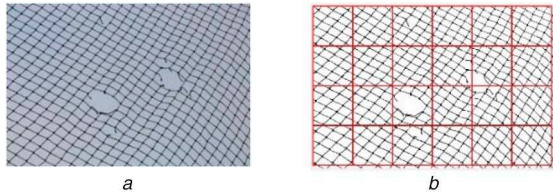


**Fig. 1** Net images  
(a) Initial net image, (b) Net image after being split into non-overlapping blocks

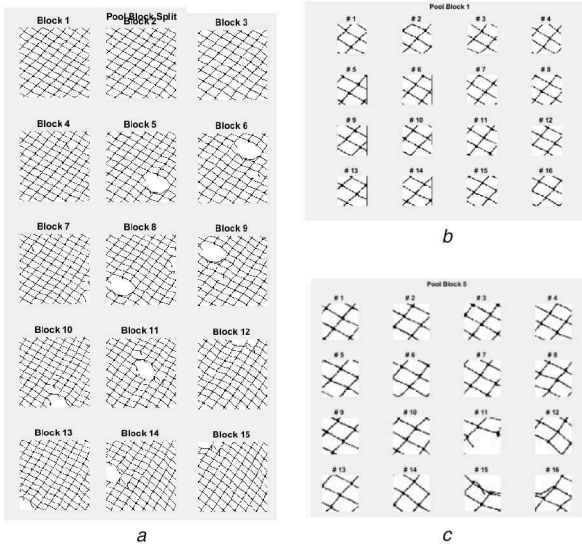


**Fig. 2** Net image split into blocks and sub-blocks  
(a) 15 blocks of net image of Fig. 1a, (b) 16 sub-blocks of block 1, (c) 16 sub-blocks of block 5

infrastructures and perform maintenance operations is the use of professional divers. However, their contribution is recommended to be as minimum as possible, while automated monitoring systems are encouraged.

As already stated, the automated monitoring system should, at least, monitor the fish cage structure for the existence of possible deformations along with any factors related to the health of the fish population. Contemporary ROV and AUV setups are equipped with one or more (in case of stereo vision) camera sensors, while they can capture video data, transfer video to an external server and, in some cases, process data on board in real-time [3–7]. The use of such systems enables actions like monitoring of fish cage nets in a regular basis.

The underwater video data processing, in both cases of online or offline assessment [8–11] is quite complex since the conditions under which data acquisition is performed cannot be fully controlled. They depend on the depth, the water currents, the presence of fishes, fouling or water formations. If we consider the specific task of monitoring the fish cage nets for discontinuities, it is clear that underwater conditions affect in a direct way the mode of net positioning, shift or rotation. For example, the same net cells are expected to differ in size and shape in successive frames because of their different pose to the camera. The detection of net discontinuities (like holes, fouling etc.) using image processing and machine vision techniques is similar to the task of detection of pattern irregularities, but with the presence of affine transformations, at least translation and rotation. Methods that use simple edge detection techniques, like Canny detector [12] or simple Hough transform [13], are not able to provide adequate results due to the temporal and spatial deformation of net cells.

Many interesting approaches have been introduced to address the irregularity in patterns. In [14], a multi-directional spatial tracking approach is proposed based on affine transformation, while in [15] texels are detected and their spatial arrangement is analysed to derive the distribution of texels for texture modelling. Other studies explore regular and near-regular textures by extracting their global periodicity using affine deformation and

Delaunay triangulation-like method [16], by manipulating the geometric, lighting and colour deformation field [17] or by computing local periodicity statistics [17].

Regarding the specific task of improving the lighting conditions using underwater image enhancement, there are state-of-the-art methods that consider light diffusion properties and illumination irregularities along with trends of image restoration methodologies [18]. In our study, we neglect the effects of depth and focus on the poor contrast of images that may be caused by absorption and scattering since we are not considering deep ocean conditions in aquaculture. More specifically, for improving contrast and sharpness, as well as for reducing non-uniform lighting of the images we test a multiplicative imaging model and apply homomorphic filtering as a preprocessing step for improving contrast and sharpness, as well as for reducing non-uniform lighting of the images [19]. Furthermore, to improve the lighting conditions we are currently experimenting with a LED source at the green–blue spectral region for reduced absorption and scattering [18]. Since the light transmission in underwater conditions does not form the main concept of this paper, we do not expand further on the formation and restoration of net images, but rather focus on the analysis of the net structure and its irregularities due to destructive damage.

So, in our study, we propose two different approaches that are suitable for in-situ monitoring and real-time application. They are based on statistical analysis and histogram considerations along with Hough transform. We aim to develop approaches that bear small computational complexity to address real-time implementation in the future, possibly performed right on the AUV.

### 3 Proposed methodology

The proposed methodology is presented as a combination of two different approaches, one based on the global distribution pattern detected via the Hough transform and another based on a statistical analysis of local intensity values. The key idea is to cover both global and local search for holes because the conditions under which the fish cage nets are operating are unpredictable even in well-structured underwater facilities. Thus, there are cases where the global image content is clear and available for processing, while others where only the local information of stretched net cells is available for processing. Furthermore, the underwater captured net images contain net cell areas along with translated, resized or rotated net cells. Our proposed fault identification scheme takes advantage of both global and local image information to cover most cases of net images. As the first step in our implementation, we test the proposed methodologies on net images presenting diverse structures of net cells, which are captured under different illumination, zoom factors and angle views conditions. For demonstration purposes, three different images are presented where the net cells differ in size and shape characteristics. These three images are common net images found in the web and they are captured under unknown to us conditions. The testing with images captured under realistic underwater conditions with equipment of known technical specifications is planned for future work.

#### 3.1 Global search for holes

The first approach is implemented through either non-overlapping or shift invariant moving window that runs all over the image with a 50% overlapping coverage from one position to another. Net hole detection results through statistical modelling of sum-distribution of net pixel intensities, to define outliers (hole positions) with a certainty based on  $p$ -values.

More specifically, every image is binarised using the Otsu threshold with black colour to represent the net lines and white colour to represent the background (Figs. 1a and b).

Then, the image is being split into larger blocks with each block covering the 25% of the total image area, while the overlapping area between blocks is set to 50%. These blocks are again being split to 16 sub-blocks each, as illustrated in Figs. 2a–c. The key idea behind this operation is to get a way to access multiple views of image blocks illustrate with similar net content.

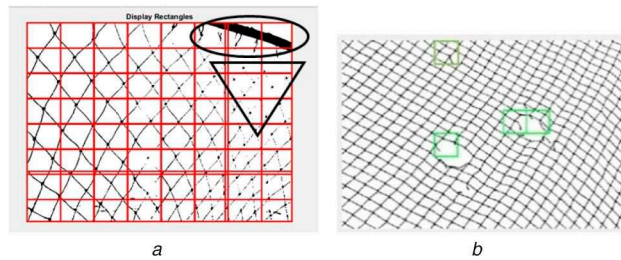
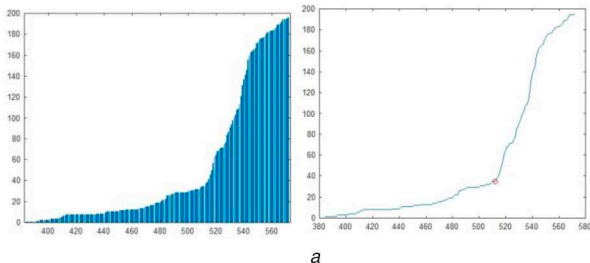
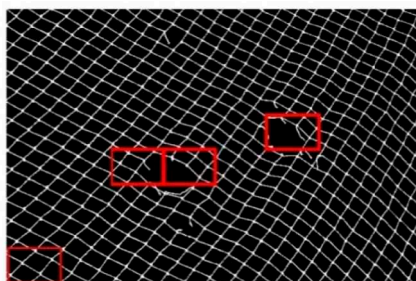


**Fig. 3** Image examples with different cdf value cases

(a) Example of cdf values  $<0.025$  in the mean distribution value (within triangle shape) and  $>0.925$   $p$ -value (within oval shape), (b) Hole net detection result



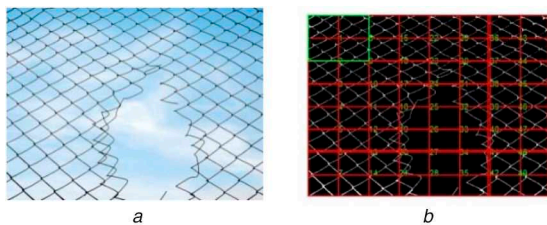
a



b

**Fig. 4** Cumulative histogram of image intensity values

(a) Cumulative histograms and threshold taking into account every image block, (b) Final result of hole detection



a

b

**Fig. 5** Example of a net image with large hole

(a) Initial image, (b) Split image result into blocks

The manipulation of the total count of net pixels (i.e. black pixels) within a block may provide a representative way to detect net holes, as this number decreases in the presence of holes. However, the absolute count of the black pixels (net line) can easily lead to erroneous conclusions, since its value under normal conditions differs drastically based on the distance from the net, its deformations, as well as the angle of viewing. It becomes obvious that an efficient normalisation scheme is necessary and to this respect, we base our proposed method on the statistical modelling of the count distribution of net pixels for the entire image.

After the split of each image to blocks (block number:  $i = [1,15]$ ) and sub-blocks (sub-block number:  $(i,j)$ ,  $j = [1,16]$ ), we calculate the normalised sum value of black pixels in each sub-block  $(i,j)$  based on the total count within the image examined. The idea behind splitting the image into subblock is to process large images in a short time using parallelism. Nevertheless, the size of each sub-block should enable capturing the basic net-cell unit, to enclosure an adequate amount of information concerning the net cells for evaluating the basic structure. For example, in Fig. 2 the net holes in sub-blocks enable capturing the irregular forms compared to the rest of the image content. Since the method can be

extended to different inspection conditions, the size of sub-blocks should be selected in relation to the image resolution, the viewing focal length and the distance from the nets. Based on different experiments the size of a sub-block should be at least two times the size of the net cell as depicted in the image of interest.

As a next step, we calculate the mean and standard deviation of net pixels within the examined image. In the next step, we formulate the histogram of block counts, forming a near-normal distribution around the calculated mean. We check the assumption of normal distribution using the Lilliefors test. Under the normality assumption, we use the 5%  $p$ -value as a significance measure for assessing whether or not the count of each sub-block may form an extreme value to the overall distribution. In the case of non-normally distributed data, first, use the Box-Cox transformation before applying the  $p$ -value test. In this test, we mostly care about the lower part of the distribution, under the 0.025  $p$ -value, which indicates the lack of pixels corresponding to the net structure. The upper extreme may indicate extreme values of large counts that may occur from severe folding and overlapping of net lines, from a drastic change in the focus point or in the distance from the net.

Overall, the count of net pixels in sub-blocks is used to define the statistic to assess extreme values. The value of each sub-block is compared against the test statistic. At the lower part of the histogram, we expect to find sub-blocks triggering the existence of irregularities (holes). At the higher part of the histogram, we identify irregularities due to reasons other than lack of net structure. Nevertheless, the lower part of the histogram can easily be misleading in the case of poor illumination conditions. Some examples of the last two cases are presented at Fig. 3. More specifically, in Fig. 3a, the case of an external (non-net) object is presented within the oval shape, whereas the case of poor imaging conditions is reflected within the triangle shape. In Fig. 3b, a result of net-hole detection is presented using the same approach.

To alleviate the false detection of holes due to a set threshold on the histogram, which might oversee low-end irregularities in the histogram distribution, we tested an alternative threshold based on the knee-point of the cumulative distribution function (cdf). For instance, if we calculate the cdf of sub-block counts corresponding to the one of Fig. 3b, then we identify a threshold value at the point of sharp increase, as in Fig. 4a. The detected image blocks where a hole or a part of it is engaged are shown in Fig. 4b. We observe here that the method can accommodate irregularities in the net structure. However, it cannot deal with very small holes due to line breaks in the net, where the broken line still appears hanging in the image. In this case, the net count will involve the same number of pixels as in the normal net formation, but some of them correspond just to broken lines. One way to overcome this limitation is to proceed with a moving window scheme instead of non-overlapping windows. This scheme would indicate large differences along the sequel of positions, triggering the existence of structural irregularity in the net weavings. In any case, the local method developed in the next section also aims to alleviate such limitations associated with the inspection of the 'gross' structure.

Figs. 5 and 6 illustrate an example of the detection process in an image with a large hole structure, whereas Figs. 7 and 8 illustrate the case of small area net hole coverage.

The blocks that are identified in Fig. 6 actually cover most of the net image area where the hole is located. Only some areas of the hole might remain undetected, as only a small part falls within a sub-block.

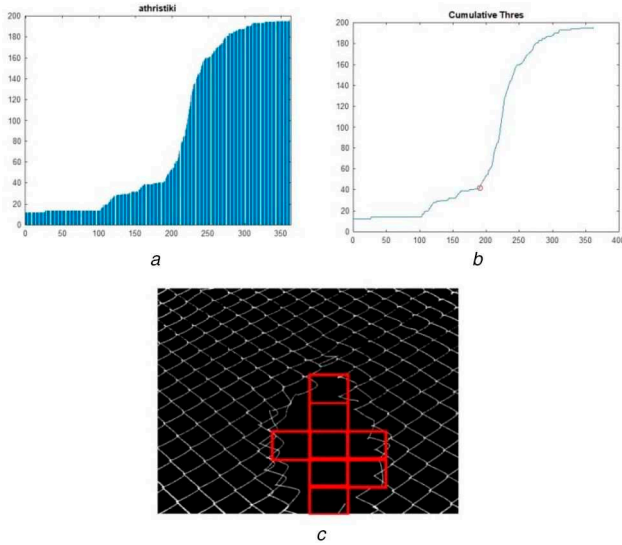


**Fig. 6** Histogram observations for net image in Fig. 5a  
 (a) Cumulative histogram, (b) Threshold determination, (c) Final result of hole detection

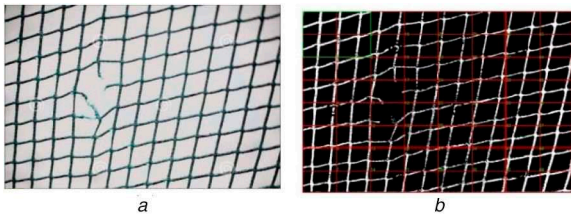


**Fig. 7** Example of a net image with small hole  
 (a) Initial image, (b) Split image result into blocks

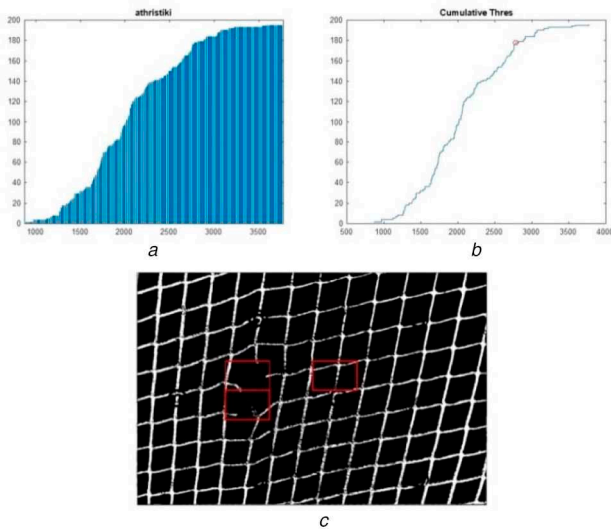


**Fig. 8** Histogram observations for net image in Fig. 7a  
 (a) Cumulative histogram, (b) Threshold determination, (c) Final result of hole detection

In the case of a net image like the one presented in Fig. 7a, the corresponding results in Fig. 8 show that the hole is detected successfully but there is also a case detected where no hole exists. This happens due to extremely poor illumination conditions that cannot be tolerated by the single threshold used. The last two problems can be dealt with an approach of moving windows instead of non-overlapping windows for the definition of sub-blocks. This scheme will achieve more detailed region coverage to capture a hole region well within the range of a sub-block, as to trigger its presence. The drawback of this implementation relates to the increased cost of operation and the increased time requirements for detection. It is a fact the AUV or ROV setups are often built

using low-level hardware or even reconfigurable logic processing to achieve (near) real-time results. Although effective processors have recently been used, the operation of a moving window could pose a serious obstacle for operations at 30 frames per second on a high-resolution wide view of the scene analysed in different scales, as highlighted in [20] for multiscale images. With the sliding window approach, the computational complexity rise to  $O(N^2M^2)$  where  $N$  is the size of a rectangular image and  $M$  the size of a rectangular window. With efficient implementation schemes, this complexity can drop down to  $O(N^2M)$  [20], which is still quite high for real-time implementation on portable low-level hardware components. Furthermore, this approach still considers a gross distribution estimation of the net lines, with multiple structures resulting to the same histogram distribution, so that it is prone to false negative errors. To resolve such ambiguity issues, we propose a net-modelling approach in the next section, based on the directionality of the net lines.

### 3.2 Local search for holes

In a local detailed view of the content of net images, we implement a methodology that models linear directions on edges via Hough transform. The idea here is to model the edge structures (net lines) with straight lined obtained from the Hough table. We expect to identify two main directions ( $\theta$ -values) with periodic repetitions in the distance axis. Since the net lines are highly deformed, we do not expect to achieve a perfect match of the model lines to the edge structures. However, the closest distance of each model point to an edge (net) pixel should be within some tolerance levels, if the net line exists. Otherwise, in the case of a net hole, we expect to identify extreme large distances, signifying empty space among model lines. The main steps of this approach are:

- Fit model lines over actual edge structures.
- Compute the distance divergence measure at each model point (from an actual edge) via the vertical distances of the model line to the closest edge.
- Perform statistical modelling of point divergences to define outliers (hole positions) with a certainty level based on  $p$ -values.

More specifically, in our approach, the Hough transform is implemented in the direction of detecting straight lines. For any line passing through the point  $(x_i, y_i)$  in the space plane, there is an equation in the polar coordinate system:

$$x \cos \theta + y \sin \theta = \rho, \quad (1)$$

where  $\rho$  represents the distance from the origin to the closest point of the line and  $\theta$  is the line orientation. For any point  $(x_i, y_i)$  on this line,  $\rho$  and  $\theta$  are constant [21]. Thus, an accumulator for each point  $(\rho, \theta)$  in the Hough space would indicate a single line in the image space.

If we plot the sinusoids described in (1) for every image pixel, then we get an image like in Fig. 9b, where the horizontal axis represents  $\theta$  and the vertical axis represents  $\rho$ . Each sinusoidal line corresponds to one edge pixel in the image domain, whereas each point in the Hough plane reflects an entire line in the image plane.

Thus, to locate the main straight lines, we need to find the main peak trends of  $\rho$  and  $\theta$  values. To this direction, we access the Hough table to get the first 100 maxima and then we estimate their CDF distribution, as in Fig. 10a. We identify the knee point of this curve as a threshold value (Fig. 10a) and we keep all values in Hough table that are higher than this as peak values. These points represent the main lines that model the image and are positioned in a narrow band around two specific values of  $\theta$ . Subsequently, we define the bands around two maxima  $\theta$  values that actually reflect the main line directions in the image using the histogram representation of the corresponding  $\theta$  values as in Fig. 10d. Furthermore, the maxima  $\rho$  values within these bands define the peaks of interest in the Hough table, indicating all lines of interest in the image across two main directions. As a result, up to this step, we have a clear estimation of  $\theta$  and  $\rho$  values of straight lines that appear in the image.

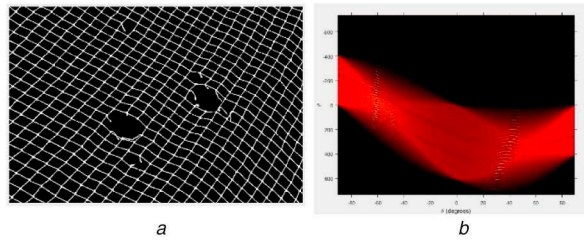


**Fig. 9** Hough table values for net image  
 (a) Initial image, (b) Hough table representing  $\theta$  values (x-axis) and  $\rho$  values (y-axis) of image lines

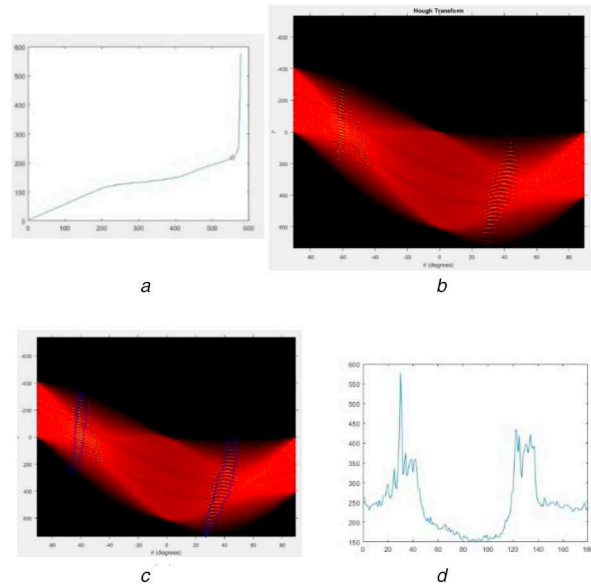


**Fig. 10** Explore Hough transform values for  $\theta$  peaks  
 (a) CDF of Hough values and Threshold for peaks in image of Fig. 9a, (b) Hough values of  $\rho$  and  $\theta$ , (c) Top maxima of two main  $\theta$  values, (d) Histogram of main  $\theta$  peaks

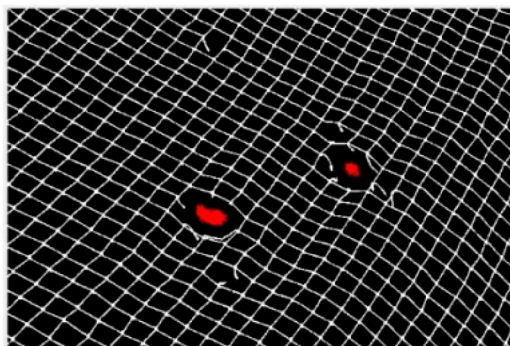


**Fig. 11** Net hole detection using the maxima of Hough transform values

As a final step, we construct all model lines reflected by the peaks in the Hough  $\theta$  and  $\rho$  values and compute the Euclidean distance from each line point to its closest edge point in the image. The histogram of distances and its extrema parts indicate the positions of net holes as in Fig. 11. The density of points within the area of holes reflects the parts of model lines within a range around the two max  $\theta$  values with extremely large distance divergence measure.

In Figs. 12 and 13, the results of two more images are presented. It becomes clear that this method detects net breaks as a means of detecting holes. This form of detection is more accurate and detailed than the former method in Section 3.1, but it poses high demands on computational complexity and time requirements. The use of low level hardware for the processing may give a way to handle these operations efficiently.

### 3.3 Proposed joint operation of fault detection schemes

In this study, we propose two methodologies for detecting holes in fish nets, stemming from different philosophies and incorporating

their particular advantages and problems. The former one is fast and strongly parallelisable, considering an abstract structure of the image based on the overall distribution of intensities. The latter method is attempting a more detailed analysis of the structure of the net, using modelling of parallel line patterns and their local distance properties. The last scheme can accomplish scrutinised search on the directionality of each net line, thus providing detailed information on the location of the line (net) breaks, but with increased requirements in time and computational complexity. To combine the properties of these two philosophies into a single integrated fault detection scheme, we propose two directions, the parallel and the sequential operation. The first one implements the simple operation of the two schemes in parallel with the combination of results at the fault detection level. The second one builds on a sequential improvement of the detection ability, with the global scheme operating first deriving the locations of the net holes, followed by the local scheme applied only in the specific local regions of the faults. Thus, the sequential application of the local scheme aims to provide detailed information about the nature

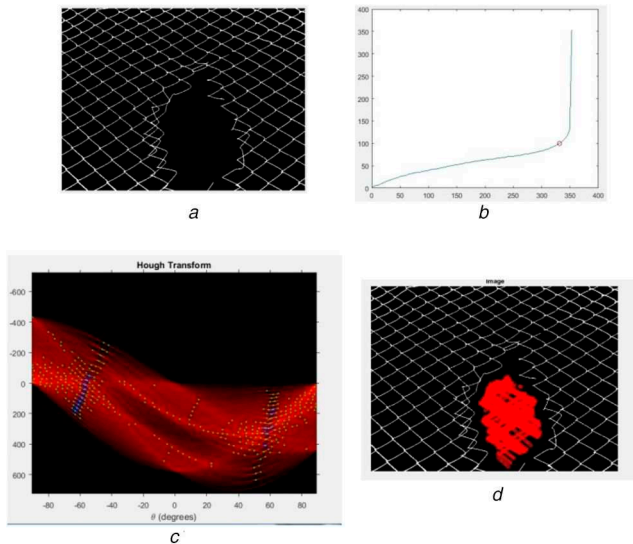


**Fig. 12** Example of a net image with large hole  
(a) Input image, (b) CDF and threshold on Hough distribution, (c) Top maxima of two main  $\theta$  values, (d) Result of net hole detection

of the fault within only a short time, since it operates only on a limited range at specific local regions rather than on the entire image.

We should notice at this point that the parallel combination pays attention to the robustness of detection since it focuses on the detection from both independent schemes. Alternatively, the sequential combination emphasises on the detailed formation of the fault (hole), as well as on the time requirements of the detection algorithm. In this study, we verified the efficiency of each individual scheme and their parallel combination, while the sequential combination is the focus of a feature study incorporating the computational requirements and the capabilities for near real-time implementation.

The combination of the two schemes is the natural consequence of our analysis, which can only improve the detection performance by exploiting both local and global geometric properties of the net structure. At this stage of development, we aim to reveal the complementarity of two different approaches, but most importantly we wish to emphasise their individual potential for the correct detection of net holes. Essentially, this study explores the potential of advanced image processing, without external lighting conditions, to resolve issues of net inspection with respect to the varying characteristics of net holes observed in difficult underwater conditions (causing affine transforms like shear, resized or rotated net cells).

## 4 Conclusions

The main objectives of this work are the detection of net holes under complex formations in terms of shape and area size. The first step of our approach relates to image pre-processing for isolating the net structure from the background colour variations, while the next steps focus on the exploitation of effective image processing techniques based on both local net structure and global image formation. The main idea behind these methods is to provide solutions for difficult underwater environment conditions during net image capture.

All images that were tested enabled successful net-hole detection. The application of the proposed two approaches support detection either in the case where the total count of net cells is clearly identified in the image or in the case where net cells appear resized or under rotation that may occur to a flexible net material.

The focus of this study was on the exploration of the detection abilities, as well as the fault diagnosis reasons for each one of the proposed schemes. The robustness of the algorithms and their combination schemes has to be routinely tested with a sequence of underwater images over time. However, the first indication of results is promising for efficiently detecting and localising net

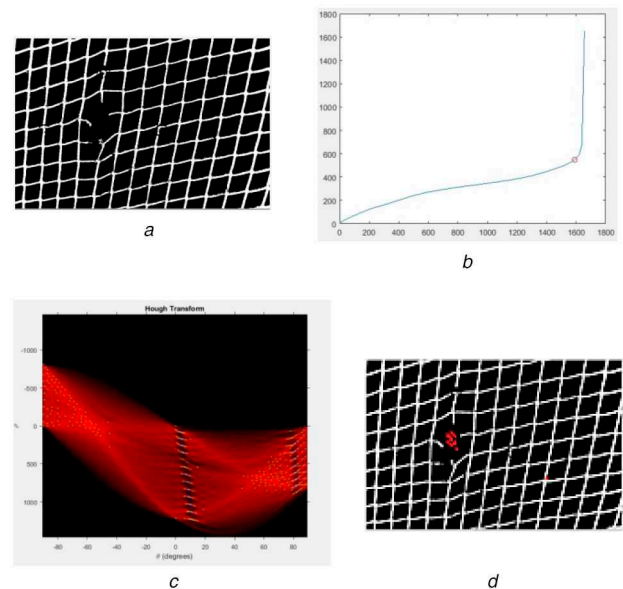


**Fig. 13** Example of a different net image with small hole at close viewing range  
(a) Input image, (b) CDF and threshold on Hough values, (c) Top maxima of two main  $\theta$  values, (d) Result of net hole detection

holes of different size, shape and image background. Future work also has to deal with the real-time implementation of the two approaches and testing on the processing unit of an ROV or AUV.

holes of different size, shape and image background. Future work also has to deal with the real-time implementation of the two approaches and testing on the processing unit of an ROV or AUV.

## 5 Acknowledgments

This work was partly implemented in the frame of the project ‘Tools for Assessment and Planning of Aquaculture Sustainability, TAPAS’ and has received funding from the EU H2020 research and innovation programme under Grant Agreement no. 678396.

## 6 References

- [1] Metian, M., Troell, M., Christensen, V., *et al.*: ‘Mapping diversity of species in global aquaculture’, *Rev Aquacult.*, 2020, **12**, pp. 1090–1100, doi: 10.1111/raq.12374
- [2] Bao, J., Li, D., Qiao, X., *et al.*: ‘Integrated navigation for autonomous underwater vehicles in aquaculture: a review’, *Information Processing in Aquaculture*, 2020, **7**, (1), pp. 139–151
- [3] Karimanzira, D., Jacobi, M., Pfuetzenreuter, T., *et al.*: ‘First testing of an AUV mission planning and guidance system for water quality monitoring and fish behavior observation in net cage fish farming’, *Inf. Process. Agric.*, 2014, **1**, pp. 131–140
- [4] Cardia, F., Lovatelli, A.: ‘Aquaculture operations in floating HDPE cages A field handbook’. FAO Fisheries and Aquaculture Technical Paper 593, Rome, Italy, 2015
- [5] Borovic, B., Vasiljevic, A., Kuljaca, O.: ‘Potentials of using underwater robotics for fishing and fish farming’. Proc. of the 10th Int. Workshop Methods for the Development and Evaluation of Maritime Technologies – DEMaT’11, Split, Croatia, 21–23 June 2011
- [6] Osen, O.L., Sandvik, R., Berge Trygstad, J., *et al.*: ‘A novel low cost ROV for aquaculture application’. OCEANS 2017, Anchorage, Anchorage, AK, 2017, pp. 1–7
- [7] Chalkiadakis, V., Papandroulakis, N., Livanos, G., *et al.*: ‘Designing a small-sized autonomous underwater vehicle architecture for regular periodic fish-cage net inspection’. 2017 IEEE Int. Conf. on Imaging Systems and Techniques (IST), Beijing, 2017, pp. 1–6, doi: 10.1109/IST.2017.8261525
- [8] Wei, C., Junfeng, W., Guannan, C., *et al.*: ‘Denoising and contrast enhancement fusion based on white balance for underwater images’. 2019 Int. Conf. on Image and Video Processing, and Artificial Intelligence, Int. Society for Optics and Photonics, Shanghai, People’s Republic of China, 2019, vol. 11321, p. 113210E
- [9] Chen, S., Wu, D., Wei, W., *et al.*: ‘An algorithm for image restoration based on underwater video series’. 2019 Int. Conf. on Modeling, Simulation, Optimization and Numerical Techniques (SMONT 2019), Atlantis Press, Shenzhen, People’s Republic of China, 2019
- [10] Siddiqui, S.A., Salman, A., Malik, M.L., *et al.*: ‘Automatic fish species classification in underwater videos: exploiting pre-trained deep neural network models to compensate for limited labelled data’, *ICES J. Mar. Sci.*, 2018, **75**, pp. 374–389
- [11] Shafait, F., Harvey, E.S., Shortis, M.R., *et al.*: ‘Towards automating underwater measurement of fish length: a comparison of semi-automatic and manual stereo-video measurements’, *ICES J. Mar. Sci.*, 2017, **74**, (6), pp. 1690–1701, <https://doi.org/10.1093/icesjms/fsx007>

- [12] Ding, L., Goshtasby, A.: 'On the canny edge detector', *Pattern Recognit.*, 2001, **34**, (3), pp. 721–725
- [13] Mukhopadhyay, P., Chaudhuri, B.B.: 'A survey of Hough transform', *Pattern Recognit.*, 2015, **48**, (3), pp. 993–1010
- [14] Leung, T., Malik, J.: 'Detecting, localizing and grouping repeated scene elements from an image'. Proc. European Conf. on Computer Vision, Cambridge, UK, 1996, pp. 546–555
- [15] Gui, Y., Ma, L.: 'Periodic pattern of texture analysis and synthesis based on texels distribution', *Vis. Comput.*, 2010, **26**, p. pp. 951–964, <https://doi.org/10.1007/s00371-010-0470-x>
- [16] Gui, Y., Chen, M., Ma, L., *et al.*: 'Texel based regular and near-regular texture characterization'. 2011, Int. Conf. on Multimedia and Signal Processing, Guilin, Guangxi, 2011, pp. 266–270, doi: 10.1109/CMSP.2011.171
- [17] Liu, Y., Lin, W.-C., Hays, J.H.: 'Near-regular texture analysis and manipulation', *ACM Trans. Graph. (SIGGRAPH 2004)*, 2004, **23**, (3), p. 368
- [18] Deng, X., Wang, H., Liu, X., *et al.*: 'Underwater image enhancement based on removing light source color and dehazing', *IEEE Access*, 2019, **7**, pp. 114297–114309, doi: 10.1109/ACCESS.2019.2936029
- [19] Garcia, R., Nicosevici, T., Cufi, X.: 'On the way to solve lighting problems in underwater imaging', *Oceans Conf.*, 2002, **2**, pp. 1018–1024, doi: 10.1109/OCEANS.2002.1192107
- [20] Hagen-Zanker, A.: 'A computational framework for generalized moving windows and its application to landscape pattern analysis', *Intl. J. Appl. Earth Obs. Geoinf.*, 2016, **44**, pp. 205–216
- [21] Gonzalez, R.C., Woods, R.E.: '*Digital image processing*' (Upper Saddle River, Prentice Hall, 2002, 2nd edn.)